



# The discrimination between phospholipids of diverse structure and phosphacoumarins of various hydrophobicity through fluorescent response of Tb-doped silica nanoparticles decorated by cationic surfactant

Olga D. Bochkova<sup>a</sup>, Asiya R. Mustafina<sup>a,\*</sup>, Alsu R. Mukhametshina<sup>b</sup>, Vladimir A. Burilov<sup>b</sup>, Andrey V. Nemtarev<sup>a,b</sup>, Vladimir F. Mironov<sup>a,b</sup>, Alexander I. Konovalov<sup>a</sup>

<sup>a</sup> A.E. Arbusov Institute of Organic and Physical Chemistry of KSC of RAS, Arbuzov Street, 8, Kazan, Russia

<sup>b</sup> Kazan (Volga region) Federal University, Kremlevskaya str. 18, 420008 Kazan, Russia

## ARTICLE INFO

### Article history:

Received 22 December 2011

Received in revised form 31 January 2012

Accepted 10 February 2012

Available online 17 February 2012

### Keywords:

Phospholipids

Silica nanoparticles

Biosensing

Luminescence

Tb(III) complex

## ABSTRACT

The work represents colloids of silica nanoparticles displaying fluorescent response on biorelevant compounds exemplified by phosphacoumarins and phospholipids. The luminescent properties of the colloids arise from Tb(III) complexes doped into silica nanoparticles (SNs). The noncovalent decoration of SNs by dicationic surfactant with further interfacial binding of dye anions enables to develop colloids programmed to display a substrate induced fluorescent response. The latter results from the quenching of Tb(III) centered luminescence by dye anions through dynamic mechanism and subsequent displacement of quenching anions by the non-quenching substrates from the interface of SNs. Both negative charge and hydrophobicity of substrates are the key factors affecting the selectivity of the substrate induced fluorescent response. The peculiar effects of zwitter-ionic and anionic phospholipids on the fluorescent response have been revealed. The applicability of the fluorescent procedure in the sensing of impurities in commercial phosphatidylcholine is also introduced.

© 2012 Elsevier B.V. All rights reserved.

## 1. Introduction

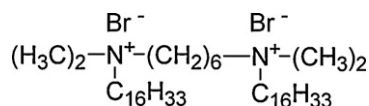
The recognition of biorelevant anions through the fluorescent response is a top of current interest [1–8]. Lanthanide-centered luminescence is of particular importance for these purposes due to narrow bands in emission spectra and long lifetimes of the excited states, which enables to get good signal-to-noise ratio [9,10]. Though literature data introduce a plenty of excellent works concerning the recognition of biorelevant anions with the use of lanthanide complexes [1–8], many problems are still unresolved. For example the lack of kinetic and thermodynamic stability of lanthanide complexes significantly restricts biocompatibility and reusability of lanthanide based molecular sensors. The encapsulation of lanthanide containing luminophores into silica nanoparticles (SNs) is a route to protect lanthanide complexes from the degradation in bio-environment [11–17]. The easy modification of SNs provides the opportunity to increase the affinity towards biotargets and biocompatibility of SNs [18,19]. The reusability of nanomaterial should be noted as an additional advantage of SNs in a bioanalytical application.

The development of nanomaterial exhibiting substrate induced fluorescent response is commonly based on the energy transfer between luminophores fixed on the silica surface or inserted into SNs and quenching molecules or ions located at the silica/water interface. The fluorescent properties of dyes are widely applied in the development of nanosized biosensors, which is well documented in the articles [20–25]. The energy transfer was successfully applied to reveal biotin–avidin binding or to detect some bio-substrates [25–27]. Though there are some fine examples of the application of lanthanide centered luminescence in the development of colloids with sensing functions [28–30,1,31,32], such publications are not enough. The peculiarity of the introduced herein approach is the discrimination between non-labeled substrates through the luminescent response with the use of dye molecules as a probe. This approach is based on the quenching of nanoparticles luminescence by some quenching ions (probes) with their further displacement by substrates, which in turn reestablishes the initial emission of nanoparticles. The previously reported use of copper or iron ions to quench the nanoparticles luminescence with further stripping of metal ions from the interface by some chelating anions should be also noted as a similar route to get substrate responsive luminescent colloids [31–33].

The present work is a continuation of our previous reports on synthesis of highly luminescent Tb(III) doped SNs [17] and

\* Corresponding author.

E-mail address: [asiyamust@mail.ru](mailto:asiyamust@mail.ru) (A.R. Mustafina).



**Scheme 1.** Hexalidene-bis(dimethylhexadecylammonium) bromide (16-6-16).

their quenching through the energy transfer mechanism by both organic and inorganic quenching ions [31,32]. It has been previously reported that the binding of sulfonephthalein dyes with surface modified Tb-doped SNs results in the quenching of Tb-centered luminescence through the energy transfer [32]. The surface decoration of SNs has been performed through the adsorption and aggregation of dicationic surfactant namely hexalidene-bis(dimethylhexadecylammonium) bromide (16-6-16, **Scheme 1**) onto silica surface with the aim to gain in the colloidal stability, biocompatibility and affinity towards anions. Sulphonephthalein dye, namely bromthymol blue has been chosen as quenching anions according to our previous results [32]. Moreover the possibility to reestablish the Tb(III) centered luminescence through the displacement of the quenching anions by nonquenching ones, which are exemplified by sodium dodecylsulfate and 1,2-distearoyl-sn-glycero-3-phospho-rac-(1-glycerol) sodium salt (DSPG) has been revealed [32]. These results can be considered as a prerequisite for a development of novel route to recognize biorelevant substrates.

Several points should be highlighted for these purposes. The first point concerns the selectivity of the displacement of quenching anions (dyes) by non-quenching ones (biorelevant anions). Thus the correlation of the substrate induced fluorescent response and the structure of substrates should be highlighted. The series of phosphocoumarins with various length of the hydrocarbon chain (**Scheme 2**) has been chosen to reveal the role of substrate hydrophobicity in the competition with dye anions. It is worth noting that the recognition of phosphocoumarins in aqueous solutions is rather appealing task due to their biological activities [34]. The applicability of the developed approach in the discrimination between phospholipids is also introduced. Phospholipids are exemplified by 1,2-distearoyl-sn-glycero-3-phospho-rac-choline (DSPC), L-phosphatidylcholine of various extent of purity (60%, 99%) and previously reported [32] 1,2-distearoyl-sn-glycero-3-phospho-rac-(1-glycerol) sodium salt (DSPG) (**Scheme 2**). It is worth noting that the application of fluorescent nanoparticles in the sensing of commercially available phosphatidylcholine (PC) with various extent of purity is rather appealing task. It is well known that extracted from egg yolk or soya bean lectin phosphatidylcholine possesses impurities, such as phosphatidylethanolamine, phosphatidylinositol, cholesterol and others [35,36]. The main route to sense and determine the above mentioned impurities are the HPLC based techniques, while the analysis of phospholipids by means of spectroscopic methods is not common. Our previous results reveal good confirmation between fluorescent response induced by SDS and DSPG and the recharging of SNs which was revealed from the electrokinetic potential data [32]. Thus the selectivity of the fluorescent response in the comparison with electrokinetic potential analysis is another key goal of the

present report. The analytical performance data, such as detection limits and dynamic linear range should be also evaluated.

## 2. Materials and methods

### 2.1. Materials

Tetraethyl orthosilicate (TEOS) 98%, ammonium hydroxide (28–30%), n-heptanol 98%, cyclohexane 99%, from Acros; terbium(III) nitrate hexahydrate (99.9%) from Alfa Aesar, Triton X-100, bromthymol blue from Sigma–Aldrich were used as purchased without further purification. Phospholipids, namely DSPC ( $\geq 98\%$ ), L- $\alpha$ -phosphatidylcholine ( $\geq 60\%$ ,  $\geq 99\%$ ), DSPG ( $\geq 97\%$ ) were used as purchased from Sigma–Aldrich without further purification.

Hexalidene-bis(dimethylhexadecylammonium) bromide 16-6-16 (**Scheme 1**) was synthesized in analogy with the procedure [37].

Phosphocoumarins (**Scheme 2**) have been synthesized according to the procedure represented in [38].

Synthesis of silica coated Tb(III) nanoparticles ( $42 \pm 5$  nm) has been performed according to reverse microemulsion procedure presented in the work [17].

### 2.2. Methods

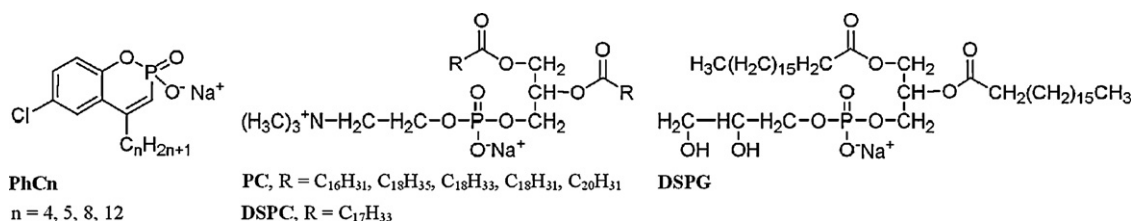
The dynamic light scattering (DLS) measurements were performed by means of the Malvern Mastersize 2000 particle analyzer. A He–Ne laser operating at 633 nm wavelength and emitting vertically polarized light was used as a light source. The measured autocorrelation functions were analyzed by Malvern DTS software and the second-order cumulant expansion methods. The effective hydrodynamic radius ( $R_H$ ) was calculated by the Einstein–Stokes relation from the first cumulant:  $D = k_B T / 6\pi\eta R_H$ , where  $D$  is the diffusion coefficient,  $k_B$  is the Boltzmann constant,  $T$  is the absolute temperature, and  $\eta$  is the viscosity. The diffusion coefficient was measured at least three times for each sample. The average error in these experiments was approximately 4%. All samples were prepared from the bidistilled water with prior filtering through the PVDF membrane using the Syringe Filter (0.45  $\mu\text{m}$ ).

Zeta potential “Nano-ZS” (MALVERN) using laser Doppler velocimetry and phase analysis light scattering was used for zeta potential measurements.

The steady-state emission spectra were recorded on a spectrofluorometer FL3-221-NIR (Jobin Yvon) under excitation at 330 nm.

Luminescence decay measurements were performed using a Horiba Jobin Yvon Fluorolog-3-221 spectrofluorometer with SPEX FL-1042 phosphorimeter accessory using a xenon flash lamp as the photon source with following parameters: time per flash–50.00 ms, flash count–200 ms, initial delay–0.05 ms and sample window–2 ms. Excitation of samples was performed at 330 nm, and emission detected at 546 nm with 5 nm slit width for both excitation and emission.

UV–vis spectra were recorded on a Lambda 35 spectrophotometer (Perkin-Elmer).



**Scheme 2.** Chemical structures of phosphocoumarines, DSPG, DSPC and PC.

All samples with nanoparticles were ultrasonicated within 30 min before measurements.

All measurements have been performed at least three times. The pH 9.2 has been adjusted by Tris (2.5 mM). Some luminescent measurements have been repeated with the use of  $\text{Na}_2\text{B}_4\text{O}_7$  (2.5 mM) at pH 9.2. This concentration of Tris is enough to maintain pH at the constant level without significant adsorption onto silica surface.

### 3. Results and discussion

#### 3.1. Electrokinetic potential and DLS measurements

The electrokinetic potential measurement is a powerful tool to reveal the aggregation of surfactants at the silica/water interface of SNs. Indeed, according to our previous results the adsorption of cationic surfactants onto SNs can be easily revealed through the recharging of SNs from  $-40$  mV to  $+30$  mV at the concentration of 16-6-16 being  $0.01$  mM. It is well known that the addition of anionic surfactant to aqueous solution of cationic micelles results in the mixed anionic–cationic aggregation, which is revealed from the recharging of micellar aggregates. The previously reported recharging of SNs at the addition of the anionic surfactant exemplified by sodium dodecylsulfate and DSPG to colloids of SNs decorated by 16-6-16 reveals the mixed anionic–cationic aggregation near the silica surface [32]. Taking into account the particular importance of hydrocarbon substituents in the aggregation of amphiphilic anions and 16-6-16, the electrokinetic potential measurements should be greatly affected by the hydrophobicity of phosphacomarins (Scheme 2). Thus electrokinetic potential measurements have been performed in colloids of SNs decorated by 16-6-16 ( $0.01$  mM) at pH 9.2 and varied concentrations of phosphacomarins. Indeed, the  $\xi$ -values represented in Fig. 1a reveal the dramatic effect of the hydrocarbon substituents on the recharging of SNs with the increase of phosphacomarins concentrations.

The  $\xi$ -value becomes close to zero, indicating the charge neutralization of SNs at the excess amounts of PhC4 (Scheme 2), while the recharging of SNs from plus to minus becomes possible in the same concentration range for more hydrophobic PhC5 (Scheme 2). The sharp decrease of  $\xi$ -values occurs for more hydrophobic PhC8 and PhC12, indicating that these anions induce efficient recharging of SNs in the narrow concentration range. Thus the more is the hydrophobicity of anions the less is their concentration required for the recharging of SNs (Fig. 1a). These results confirm that the recharging of SNs derives from the mixed cationic–anionic aggregation at their interface. Though the interfacial aggregation behavior follows the well known tendency for the mixed aggregation in aqueous solutions [39,40], some difference from the aggregation in the bulk of solution should be noted. The  $\xi$ -values of SNs with the further concentration growth of PhC8 and PhC12 tend to come to the plateau, indicating no further recharging of SNs at these conditions (Fig. 1a), while the charge of the mixed aggregates in aqueous solutions follows the molar ratio of cationic and anionic surfactants (Table 1S in Suppl. Data). The high initial charge of SNs at pH 9.2 ( $-45$  mV [32]) should be mentioned as the main reason of this difference. Indeed the mixed cationic–anionic aggregation near the negatively charged silica surface should differ from the similar aggregation in the bulk of solution [41]. The saturated levels of the curves are not the same for PhC12 and PhC8 (Fig. 1a), indicating the correlation between the recharging of SNs and the hydrophobicity of the competitive anions. The experimentally observed recharging of SNs reflects the efficiency of the mixed cationic–anionic aggregation near the silica surface, which is quite different from that in the bulk of solution. The aggregation behavior of SNs follows their

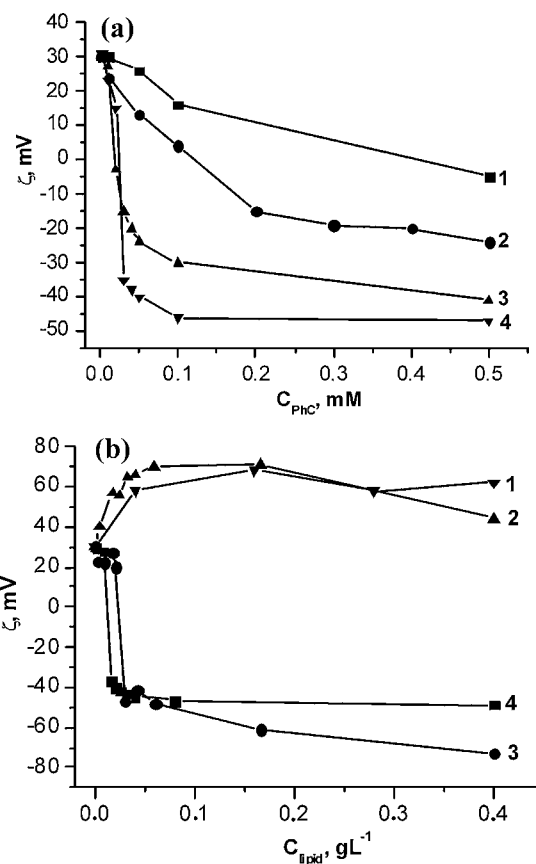


Fig. 1. The  $\zeta$ -potential value of Tb(III) doped SNs ( $C = 0.028$   $\text{g L}^{-1}$ ) at  $0.01$  mM of 16-6-16 and various amounts of (a): phosphacomarins PhC4 (1), PhC5 (2), PhC8 (3) and PhC12 (4) ( $\text{SD} = 5$  mV,  $n = 3$ ) and (b): lipids DSPC (1) ( $\text{SD} = 15$  mV,  $n = 3$ ), PC 99% (2) ( $\text{SD} = 15$  mV,  $n = 3$ ), PC 60% (3) ( $\text{SD} = 5$  mV,  $n = 3$ ) and DSPG (4) ( $\text{SD} = 5$  mV,  $n = 3$ ) at pH 9.2.

electrokinetic potential values, being more enhanced in the narrow concentration range where  $\xi$  potential values are close to zero and coming to nothing at enhanced positive and negative  $\xi$  values (Table 2S in Suppl. Data). Thus the aggregation behavior of SNs is guided by the mixed aggregation of 16-6-16 with the hydrophobic anions at the silica/water interface.

The tendency of phospholipids to form mixed aggregates with cationic surfactants [42–44], as well as to aggregate onto silica surface pretreated by organic ions is well known [45–49]. Fig. 1b represents the  $\xi$ -values at the various concentrations of phospholipids, including previously reported DSPG for the comparison. The profiles of the curves for DSPG and PC (60%) practically coincide with each other, indicating the recharging of SNs from plus to minus (Fig. 1b). No silica surface recharging is observed with the increase of PC (99%) and DSPC concentrations. Moreover the  $\xi$ -values tend to become more positive with their concentrations increase (Fig. 1b). The zwitter ionic structure derived from the presence of ammonium group in the structures of PC and DSPC can be considered as the explanation of the observed increase of  $\xi$ -values. Thus the decrease of  $\xi$ -potential induced by PC (60%) can be assumed as an indication of the anionic impurities such as phosphatidylethanolamine [35,36], which is predominantly in the anionic form at pH 9.2 and thus tends to form mixed aggregates with 16-6-16. The participation of the anionic impurities in the mixed aggregation can be assumed as the most probable reason of the recharging of SNs in solutions of PC(60%), making the profile of  $\xi$ -values versus concentration being quite similar with that of DSPG.

### 3.2. Steady state and time resolved luminescence measurements

The insertion of Tb(III) complexes into SNs (about 5000 in each SN [17]) results in high luminescence intensity of their aqueous dispersions. Thus concentration of SNs being  $0.028 \text{ g L}^{-1}$  ( $7 \times 10^{-10} \text{ M}$ , the way of calculation is represented in [17]) is maintained in all fluorimetric measurements. No leakage of luminophores from SNs to aqueous media is observed within rather long time (one week at least [17]), which is the prerequisite condition for their analytical application. The emission spectra of SNs in aqueous solution (Fig. 1S in Suppl. Data) is common for Tb-centered luminescence with four bands, where the peak at 541 nm assigned to  $^5\text{D}_4\text{-}^7\text{F}_5$  transition is the main [9,17]. The main peak intensity is applied as the intensity of Tb-centered luminescence. The previous results reveal the conditions of the efficient energy transfer between silica coated Tb(III) complexes and bromthymol blue (BThB) anions, which are pH 9.2, 0.01 mM of BThB and 0.01 mM of 16-6-16 [32]. These pH and concentration conditions enable to keep the energy acceptors (anions of BThB) in close proximity to silica coated energy donors (Tb(III) complexes). The inner filter effect of BThB should be mentioned as the reason of the suppressed steady state luminescence [32]. This effect is also kept on the constant and insignificant level at various concentrations of phosphacoumarins PhC4, PhC5, PhC8 (Fig. 2S–4S, Suppl. Data), excepting PhC12, where the absorption at 541 nm is somewhat raised due to the baseline lift (Fig. 4S, Suppl. Data). The latter derives from the enhanced scattering due to formation of large cationic–anionic aggregates in the bulk of solution (Tables 1S, 2S in Suppl. Data). Both steady state and time resolved measurements have been performed to reveal the effect of various phosphacoumarins on the emission intensity ( $I$ ) and lifetimes ( $\tau$ ) of SNs decorated by 16-6-16 in the presence of BThB at varied concentrations of phosphacoumarins and phospholipids. The obtained data are represented in Figs. 2 and 3 in the relative forms, which are  $\tau/\tau_0$  and  $I/I_0$ , where  $\tau_0$  and  $I_0$  designates the lifetime and emission intensity of the aqueous dispersion of SNs without dye. The single point designated as “+BThB” in Figs. 2a and 3a indicates the  $I/I_0$  value of SNs at 0.01 mM of BThB without 16-6-16 at the same pH conditions. It is worth mentioning that this value is less than 1 due to the inner filter effect of BThB.

Both steady state and time resolved measurements (Fig. 2) reveal the insignificant effect of PhC4 and PhC5 on the quenching of Tb-centered luminescence by BThB, indicating that both anions provide rather poor displacement of BThB from the interface of SNs. The addition of both PhC8 and PhC12 provides the significant increase of  $\tau/\tau_0$  and  $I/I_0$ . The increase of  $\tau/\tau_0$  ( $I/I_0$ ) values comes to the saturation level for both PhC8 and PhC12. Though the slopes of  $\tau/\tau_0$  and  $I/I_0$  versus concentration of PhC12 coincide with those of PhC8, the corresponding saturation levels differ from each other. The addition of PhC12 provides the reestablishment of  $\tau/\tau_0$  to 1 and  $I/I_0$  to the value designated as “+BThB” at rather diluted concentration conditions, while the reestablishment is not whole for PhC8. It is worth noting that the quenching measurements are in rather good correlation with the electrokinetic potential data (Figs. 1 and 2). So, the more is the hydrophobicity of the competitive anion the more is the displacement of the quenching anions and the reestablishment of Tb-centered luminescence. This fact prompts us to reveal the effect of more hydrophilic anions, such as  $\text{HPO}_4^{2-}$  on the quenching measurements at the same conditions. The obtained spectral data (Fig. 1S in Suppl. Data) indicate no effect of hydrophilic phosphates on the quenching measurements. Thus hydrophilic anions including those arising from the use of buffer systems do not interfere with the recognition of hydrophobic anions, which is of great importance for practical application. So the slopes of  $\tau/\tau_0$  and  $I/I_0$  versus concentration of phosphacoumarins indicate the key role of the hydrophobic tail in the displacement of BThB by hydrophobic anions from the interface of SNs decorated

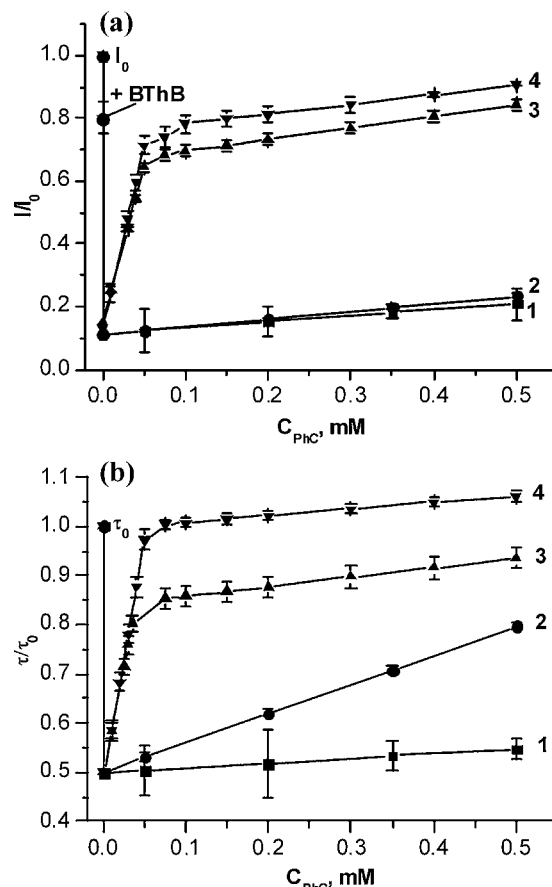
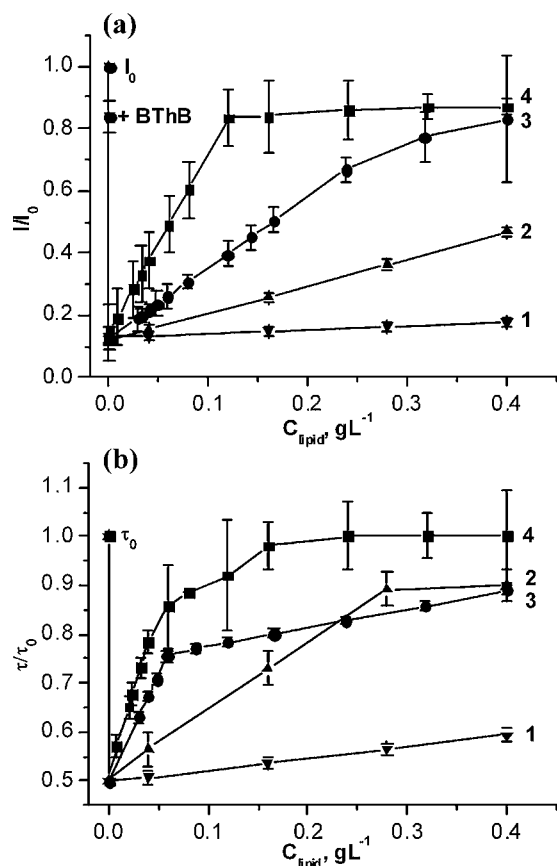


Fig. 2. The  $I/I_0$  (a) and  $\tau/\tau_0$  (b) of Tb(III) doped SNs ( $C=0.028 \text{ g L}^{-1}$ ) at 0.01 mM of 16-6-16, 0.01 mM of BThB and various concentrations of phosphacoumarins: PhC4 (1), PhC5 (2), PhC8 (3) and PhC12 (4) at pH 9.2;  $I_0$  and  $\tau_0$  are the emission intensity and lifetime without dye correspondingly. The  $I/I_0$  value without 16-6-16 and phosphacoumarins is designated as “+BThB”.

by 16-6-16. Though the steady state and time resolved quenching measurements correlate with each other some difference between them is worth noting. For example the curves  $I/I_0$  versus concentration are very close to each other for PhC4 and PhC5, while the concentration growth provides greater increase of  $\tau/\tau_0$  for PhC5 in the comparison with PhC4. The discrepancy between the steady state and time resolved quenching measurements is less enhanced but is still detectable in the case of PhC8 and PhC12. These discrepancies arise from the diverse inner filter and light scattering effects. The various inner filter effects result from the absorbance of BThB in micellar solutions which in turn is affected by the charge and morphology of the micellar aggregates [50]. The spectra of BThB in solutions of SNs decorated by 16-6-16 at various concentrations of phosphacoumarins are represented in Figs. 2S–4S (Suppl. Data). The light scattering effect should be also noted as another possible reason of the restricted emission intensities. This effect is evident from the baseline lift at the increased concentration of PhC12 (Fig. 4S, Suppl. Data). Thus the time resolved quenching measurements which are independent on inner filter and light scattering effects more really reflect the displacement of quenching ions by phosphacoumarins of various hydrophobicity.

The previously published results reveal DSPG molecules as efficient competitors of BThB for interfacial binding with SNs [32], which is evident from the reestablishment of both  $\tau/\tau_0$  and  $I/I_0$  in the narrow concentration range. No significant increase of the both values is observed at the addition of DSPG (Fig. 3).

Taking into account literature and electrokinetic potential data represented in Fig. 1b DSPG molecules are efficiently adsorbed onto



**Fig. 3.** The  $I/I_0$  (a) and  $\tau/\tau_0$  (b) of Tb(III) doped SNs ( $C=0.028\text{ g L}^{-1}$ ) at 0.01 mM of 16-6-16, 0.01 mM of BThB and various concentrations of phospholipids: DSPC (1), PC 99% (2), PC 60% (3) and DSPG (4) at pH 9.2.  $I_0$  and  $\tau_0$  are the emission intensity and lifetime without dye correspondingly. The  $I/I_0$  value without 16-6-16 and lipids is designated as “+BThB”.

interface of SNs decorated by 16-6-16, while this adsorption does not lead to the displacement of BThB. Though both DSPC and PC molecules are zwitterionic, their addition in similar concentration conditions provides different fluorescent response (Fig. 3). It is rather unexpected that the addition of PC (99%) provides more enhanced displacement of BThB than DSPC (99%). The observed difference may arise from the various structures of the hydrophobic substituents of PC and DSPC (R in Scheme 2). The different content of the impurities in both DSPC (99%) and PC (99%) should be also taken into account as the probable reason of this difference. The enhanced fluorescent response resulted from the addition of PC (60%) confirms that the more is the percentage of the anionic impurities the more is the fluorescent response of SNs on the addition of the commercial phospholipids. The discrepancy between the steady state and time resolved quenching measurements for phospholipids is also worth noting (Fig. 3a and b). The dynamic light scattering data represented in Tables 1S, 2S (Suppl. Data) indicate the significant self and mixed aggregation of PC (99 and 60%) and DSPC in the studied solutions. The analysis of the absorbance spectra of the multicomponent solutions (SNs, 16-6-6, BThB) at various concentrations of phospholipids (Figs. 5S–7S) indicates the significant baseline lift arisen from the aggregation of phospholipids. These light scattering effects resulted from the mixed and self aggregation of phospholipids in turn should affect the emission intensity at 541 nm. Though the time resolved quenching measurements more really reflect the displacement of quenching ions, the  $I/I_0$  values exhibit better sensitivity to the structure and greater linear ranges for the studied phospholipids (Fig. 3). Thus the steady

**Table 1**

The detection limits (DL) and dynamic linear ranges (DLR) for PhC8 and PhC12 (mM), as well as for DSPG and PC with various extent of purity (99% and 60%) in  $\text{g L}^{-1}$ .

| Substrate        | PhC8       | PhC12      | DSPG                    | PC(99%)                | PC(60%)                |
|------------------|------------|------------|-------------------------|------------------------|------------------------|
| DL <sup>a</sup>  | 0.005 mM   | 0.005 mM   | 0.008 $\text{g L}^{-1}$ | 0.05 $\text{g L}^{-1}$ | 0.02 $\text{g L}^{-1}$ |
| DLR <sup>a</sup> | 0.005–0.05 | 0.005–0.05 | 0.008–0.04              | 0.05–0.4               | 0.02–0.23              |

<sup>a</sup> The DL and DLR values are evaluated from the steady state quenching measurements.

state quenching measurements have been used to evaluate detection limits and dynamic linear ranges of the phospholipids (Table 1).

The analysis of electrokinetic potential data in the correlation with the steady state and time resolved quenching measurements reveals good correlation between them for phosphacoumarins. Thus the hydrophobicity of anions greatly affects their mixed aggregation with cationic surfactant at the silica/water interface, resulting in both the recharging of SNs and the displacement of BThB anions. The abrupt linear increase of  $\tau/\tau_0$  and  $I/I_0$  occurring within 0–0.05 mM of PhC8 and PhC12 is the basis of their quantitative determination in solution, though their detection limits are the same (Table 1). The comparative analysis of the electrokinetic and luminescent data for phospholipids indicate that anionic phospholipids can be easily distinguished from the zwitterionic ones through both fluorescent and electrokinetic potential measurements. It is worth noting that DSPG and PC (60%), as well as DSPC and PC (99%) can not be distinguished through electrokinetic potential data, while each of them provide its own profile of the steady state and time resolved luminescent response with various detection limits and linear ranges (Figs. 1 and 3, and Table 1).

The obtained results enable to highlight the main structural features of the determinate substrates which guide the selectivity of the substrate induced luminescent response. First of all the substrate should be enough hydrophobic. This factor derives from the binding mode between the probe molecules and SNs, which is the penetration of the hydrophobic anions namely BThB into the micellar adlayer at the silica/water interface. Thus hydrophilic anions do not interfere with the recognition of hydrophobic ones, which enables to use any buffer system as the background (no difference has been revealed between Tris and  $\text{Na}_2\text{B}_4\text{O}_7$  buffer systems). The role of the charge of the determinate substrate is dramatic but not so crucial. In particular zwitterionic amphiphilic molecules also participate in the mixed aggregation with dicationic surfactant molecules, though no recharging of the aggregates occurs in this case. Thus the insignificant displacement of the dye anions is induced by this aggregation. This is the reason of the discrimination between the anionic and zwitterionic phospholipids, as well as between PC and its anionic impurities.

#### 4. Summary

The obtained results introduce the novel route to discriminate between hydrophobic and hydrophilic biorelevant anions through the off-on switching of the Tb(III)-centered luminescence with the use of luminescent Tb-doped silica nanoparticles decorated by cationic surfactant and bromthymol blue as a probe. The selectivity of the substrate induced fluorescent response is controlled by the charge of the substrates and the structure of their hydrophobic substituents. Thus sodium salts of phosphacoumarins with  $\text{C}_{12}\text{H}_{25}$  and  $\text{C}_8\text{H}_{17}$  induce the fluorescent response in more diluted conditions than their less hydrophobic counterparts, while hydrophilic anions such as arisen from the buffer systems provide poor interference with hydrophobic substrates. The analysis of the fluorescent response arisen from the addition of phospholipids indicates that anionic phospholipids can be recognized through the fluorescent response versus the zwitterionic ones. Moreover the presence

and the quantity of the anionic impurities in zwitter ionic phosphatidylcholine can be revealed through the fluorescent response of Tb-doped silica nanoparticles. The represented approach exemplifies the luminescent sensing of anionic phospholipids, which is not common itself. Moreover further development of this approach may result in a new procedure to sense the formation of phospholipids membranes onto silica templates. This work is in progress now.

### Acknowledgement

We thank RFBR (projectN 10-03-00352-a) for financial support.

### Appendix A. Supplementary data

Supplementary data associated with this article can be found, in the online version, at doi:10.1016/j.talanta.2012.02.023.

### References

- [1] B.C. Barja, P.F. Aramendria, Photochem. Photobiol. Sci. 7 (2008) 1391–1399.
- [2] C. Tan, Yu. Zheng, Q. Wang, W. Zhang, S. Zheng, S. Cai, J. Fluoresc. (2010), doi:10.1007/s10895-010-0787-x.
- [3] J. Massue, S.J. Quinn, T. Gunnlaugsson, J. Am. Chem. Soc. 130 (2008) 6900–6901.
- [4] C.G. Gulgas, T.M. Reineke, Inorg. Chem. 47 (2008) 1548–1559.
- [5] H.A. Azab, S.A. El-Korashy, Z.M. Anwar, B.H.M. Hussein, G.M. Khairy, Spectrochim. Acta A 75 (2010) 21–27.
- [6] S. Khatua, S.H. Choi, J. Lee, K. Kim, Y. Do, D.G. Churchill, Inorg. Chem. 48 (2009) 2993–2999.
- [7] S.E. Plush, T. Gunnlaugsson, Dalton Trans. 29 (2008) 3801–3804.
- [8] J.P. Leonard, C.M.G. Dos Santos, S.E. Plush, T. McCabe, T. Gunnlaugsson, Chem. Commun. 2 (2007) 129–131.
- [9] S.V. Eliseeva, J.-C.G. Bünzli, Chem. Soc. Rev. 39 (2010) 189–227.
- [10] J. Shen, L.-D. Sun, C.-H. Yan, Dalton Trans. (2008) 5687–5697.
- [11] F. Enrichi, R. Ricco, P. Scopece, A. Parma, A.R. Mazaheri, P. Riello, A.J. Benedetti, Nanopart. Res. 12 (2010) 1925–1931.
- [12] F. Gao, F. Luo, X. Chen, W. Yao, J. Yin, Zh. Yao, L. Wang, Talanta 80 (2009) 202–204.
- [13] H. Jiang, G. Wang, W. Zhang, X. Liu, Z. Ye, D. Jin, J. Yuan, Zh. Liu, Fluorescence 20 (2010) 321–328.
- [14] K. Binnemans, P. Lenaerts, K. Driesen, Ch. Görller-Walrand, J. Mater. Chem. 14 (2004) 191–195.
- [15] Ch. Wu, J. Hong, X. Guo, Ch. Huang, J. Lai, J. Zheng, J. Chen, X. Mu, Y. Zhao, Chem. Commun. (2008) 750–752.
- [16] H. Härmä, Ch. Graf, P. Hänninen, J. Nanopart. Res. 10 (2008) 1221–1224.
- [17] A.R. Mustafina, S.V. Fedorenko, O.D. Konovalova, A.Yu. Menshikova, N.N. Shevchenko, S.E. Soloveva, A.I. Konovalov, I.S. Antipin, Langmuir 25 (2009) 3146–3159.
- [18] Y. Wang, Y. Yan, J. Cui, L. Hosta-Rigau, J.K. Heath, E.C. Nice, F. Caruso, Adv. Mater. 22 (2010) 4293.
- [19] A.S. de Dios, M.E. Díaz-García, Anal. Chim. Acta 666 (2010) 1–22.
- [20] S. Bonacchi, D. Genovese, R. Juris, E. Marzocchi, M. Montalti, L. Prodi, E. Rampazzo, N. Zaccheroni, in: C.D. Geddes (Ed.), Reviews in Fluorescence, Springer Inc., Baltimore, 2008, pp. 119–137.
- [21] M. Montalti, L. Prodi, N. Zaccheroni, A. Zattoni, P. Reschiglian, G. Falini, Langmuir 20 (2004) 2989–2991.
- [22] R.P. Bagwe, C. Yang, L.R. Hilliard, W. Tan, Langmuir 20 (2004) 8336–8342.
- [23] S. Bonacchi, E. Rampazzo, M. Montalti, L. Prodi, N. Zaccheroni, F. Mancin, P. Teolato, Langmuir 24 (2008) 8387–8392.
- [24] C. He, W. Zhu, Yu. Xu, Ye. Zhong, J. Zhou, X. Qian, J. Mater. Chem. 20 (2010) 10755–10764.
- [25] S.M. Saleh, R. Ali, T. Hirsch, O.S. Wolfbeis, J. Nanopart. Res. 398 (2010) 1615–1623.
- [26] Ya. Wang, Yu. Wang, B. Liu, Nanotechnology 19 (2008) 415605, doi:10.1088/0957-4484/19/41/415605.
- [27] D.R. Larson, H. Ow, H.D. Vishwasrao, A.A. Heikal, U. Wiesner, W.W. Webb, Chem. Mater. 20 (2008) 2677–2684.
- [28] J.-Q. Gu, J. Shen, L.-D. Sun, C.-H. Yan, J. Phys. Chem. 112 (2008) 6589–6593.
- [29] S. Pihlasalo, J. Kirjavainen, P. Hänninen, H. Härmä, Anal. Chem. 83 (2011) 1163–1166.
- [30] H. Dong, Ya. Liu, D. Wang, W. Zhang, Z. Ye, G. Wang, J. Yuan, Nanotechnology 21 (2010) 395504, doi:10.1088/0957-4484/21/39/395504.
- [31] V. Skripacheva, A. Mustafina, N. Davydov, V. Burilov, A. Konovalov, S. Soloveva, I. Antipin, Mater. Chem. Phys. 132 (2012) 488–493.
- [32] O.D. Bochkova, A.R. Mustafina, A.R. Mukhametshina, V.A. Burilov, V.V. Skripacheva, L. Ya Zakharova, S.V. Fedorenko, A.I. Konovalov, S.E. Soloveva, I.S. Antipin, J. Colloids Surf. B 92 (2012) 327–333.
- [33] S. Seo, H.Y. Lee, M. Park, J.M. Lim, D. Kang, J. Yoon, J.H. Jung, Eur. J. Inorg. Chem. (2010) 843–847.
- [34] X. Li, D. Zhang, H. Pang, F. Shen, H. Fu, Y. Jiang, Y. Zhao, Org. Lett. 7 (2005) 4919–4922.
- [35] K. Teubera, J. Schiller, B. Fuchs, M. Karas, T.W. Jaskolla, Chem. Phys. Lipids 163 (2010) 552–560.
- [36] W. Gladkowski, A. Chojnacka, G. Kielbowicz, T. Trziszka, C. Wawrzenczyk, J. Am. Oil Chem. Soc. (2011), doi:10.1007/s11746-011-1893-x.
- [37] A. Mirgorodskaya, L. Kudryavtseva, V. Pankratov, S. Lukashenko, L. Rizvanova, A. Konovalov, J. Gen. Chem. 76 (2006) 1696–1701.
- [38] I.S. Ryzhkina, L.I. Murtazina, A.V. Nemtarev, V.F. Mironov, A.I. Konovalov, Mendeleev Commun. 20 (2010) 148–150.
- [39] P.M. Holland, D.N. Rubingh, in: P.M. Holland, D.N. Rubingh (Eds.), Mixed Surfactant Systems, ACS Inc., Washington, 1992, pp. 2–30.
- [40] R. Nagarajan, Adv. Colloid Interface Sci. 26 (1986) 205–264.
- [41] S. Manne, G. Warr, Supramolecular Structure in Confined Geometries. Supramolecular Structure of Surfactants Confined to Interfaces, ACS, Washington, DC, 1999 (Chapter 1).
- [42] M.B. Singh, K. Singh, J. Singh, J. Colloid Interface Sci. 297 (2006) 284–291.
- [43] M.B. Singh, J. Singh, G. Kaur, Chem. Phys. Lipids 138 (2005) 81–92.
- [44] A. Brun, G. Brezesinski, H. Möhwald, M. Blanzat, E. Perez, I. Rico-Lattes, Colloids Surf. A: Physicochem. Eng. Aspects 228 (2003) 3–16.
- [45] E. Chibowski, A.V. Delgado, K. Rudzka, A. Szczes, L. Hołysz, J. Colloid Interface Sci. 353 (2011) 281–289.
- [46] G. Gopalakrishnan, I. Rouiller, D.R. Colman, R.B. Lennox, Langmuir 25 (2009) 5455–5458.
- [47] R. Rapuano, A.M. Carmona-Ribeiro, J. Colloid Interface Sci. 226 (2000) 299–307.
- [48] S.P. Moura, A.M. Carmona-Ribeiro, Langmuir 21 (2005) 10160–10164.
- [49] R. Rapuano, A.M. Carmona-Ribeiro, J. Colloid Interface Sci. 193 (1997) 104–111.
- [50] N. Mchedlov-Petrosyan, Pure Appl. Chem. 80 (2008) 1459.